Chemical Engineering Journal 245 (2014) 107–116

Contents lists available at ScienceDirect

Chemical Engineering Journal

journal homepage: www.elsevier.com/locate/cej

Selective oxidation of aromatic alcohols to corresponding aromatic aldehydes using In_2S_3 microsphere catalyst under visible light irradiation

Mengli Xie [a], Xia Dai [a], Sugang Meng [a], Xianliang Fu [a], Shifu Chen [a,b,*]

[a] Department of Chemistry, Huaibei Normal University, Huaibei 235000, Anhui, People's Republic of China
[b] Department of Chemistry, Anhui Science and Technology University, Fengyang 233100, Anhui, People's Republic of China

HIGHLIGHTS

- In_2S_3 microsphere with E_{CB} = −0.78 eV and E_{VB} = 1.18 eV was prepared.
- In_2S_3 has an excellent performance for the conversion of aromatic alcohols.
- The conversion is 41.5% and the yield is 41.4% after being illuminated for 4 h.
- $\cdot O_2^-$ and ·OH are the important oxidizing agents in the selective oxidation process.

GRAPHICAL ABSTRACT

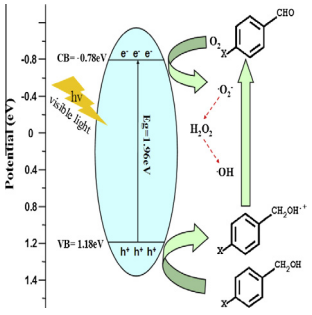

ARTICLE INFO

Article history:
Received 8 December 2013
Received in revised form 5 February 2014
Accepted 11 February 2014
Available online 17 February 2014

Keywords:
Selective oxidation
Aromatic alcohols
In_2S_3
Visible light
Mechanism

ABSTRACT

Selective oxidation has become an alternative green way for organics synthesis and environmental remediation. In this paper, selective oxidation of aromatic alcohols to corresponding aromatic aldehydes under visible light irradiation using In_2S_3 microsphere as a photocatalyst was investigated. In_2S_3 microsphere with a band gap of 1.96 eV was prepared by using $InCl_3{\cdot}4H_2O$ and CH_3CSNH_2 as precursor. The structure and optical properties of In_2S_3 photocatalyst were investigated by X-ray powder diffraction, UV–vis diffuse reflectance spectroscopy, scanning electron microscopy, transmission electron microscopy, energy-dispersive spectroscopy, nitrogen adsorption–desorption and photoluminescence spectra. The results showed that the In_2S_3 microsphere has an excellent photocatalytic performance in the conversion of aromatic alcohols to corresponding aromatic aldehydes. For selective oxidation of benzyl alcohol, when illumination time is 4 h, the conversion reaches to 41.5%, and the yield is 41.4%. In_2S_3 microsphere as a photocatalyst has a good stability when it was used 5 times for selective oxidation of benzyl alcohol. $\cdot O_2^-$ and ·OH are the important oxidizing agents in the photocatalytic process. The possible mechanism for the conversion of aromatic alcohols to corresponding aromatic aldehydes was proposed.

© 2014 Elsevier B.V. All rights reserved.

1. Introduction

It is known that environmental pollution and energy crisis have been the crucial problems that influence the progress of world economy. Because photocatalysis can be applied to waste water treatment, environmental modification, producing hydrogen from water splitting and selective transformation of organics, etc., it has been attracting much attention in recent years. Among them, selective oxidation of alcohols to corresponding aldehydes without further oxidation to carboxylic acids and carbon dioxide has become a research hotspot recently [1–3]. Aromatic aldehydes and their derivatives are important fine chemical intermediates, which

* Corresponding author at: Department of Chemistry, Huaibei Normal University, Huaibei 235000, Anhui, People's Republic of China. Tel.: +86 561 3806611; fax: +86 561 3090518.
E-mail address: chshifu@chnu.edu.cn (S. Chen).

http://dx.doi.org/10.1016/j.cej.2014.02.029
1385-8947/© 2014 Elsevier B.V. All rights reserved.

have been widely used in the synthesis of spices, alcoholic beverage, drugs etc. At present, in order to obtain these aromatic aldehydes in the industrial manufacture, the stoichiometric oxidizing agents, such as $KMnO_4$, MnO_2, RuO_4, CrO_3, ClO^- and Br_2 are used in the process of selective oxidation. However, it can produce the equivalent of metal waste and cause environmental pollution [4,5]. So, searching for an environmentally friendly way to replace the conventional methods of selective oxidation is of great significance. Therefore, the development of oxygen oxidation technology, which is helpful for conversion of alcohol to aldehyde, has the vital significance in environmental protection [6–8].

It has been reported that semiconductor photocatalysts can be applied in the selective oxidation of $-CH_2OH$ to $-CHO$ instead of CO_2 and H_2O. Titanium oxide (TiO_2) has been acknowledged as one of the most promising photocatalysts in many fields because of its low cost, physical and chemical stability, high photocatalytic activity and easy availability [9,10]. It is known that TiO_2 has strong oxidation ability and cannot make full use of visible light due to its positive valence band of 2.7 eV and wide energy gap of 3.2 eV (vs. NHE pH 7). It has been proved that TiO_2 can oxidize all organics to carbon dioxide, water and mineral acid, which cannot achieve the selective oxidation of alcohols to aldehydes under the presence of UV light and oxygen. Therefore, titanium dioxide and other broadband materials are not suitable as photocatalysts for the selective oxidation of organics. In order to improve the selective oxidation performance, a series of modification of TiO_2 have been explored [8,11–14], such as graphene–TiO_2 [15], M/TiO_2 (M = Au, Pd, Pt) [16] and so on [17–19]. Furthermore, Zhang and coworkers have researched the aerobic oxidation of alcohols to corresponding aldehydes which has high selectivity using a special coupled system consisting of dye-sensitized TiO_2 and TEMPO (2,2,6,6-tetramethypiperdinyloxyl) under visible light illumination [8]. At the same time, other composite photocatalysts, such as Pd@CeO_2 [20], Pt@CeO_2 [21] and Au/CeO_2 [22], have also been reported for the selective oxidation of alcohols to aldehydes or ketones. Although it has made a great progress in conversion and selectivity, it is still far from what is expected.

The crux of the problem lies in how to design and prepare photocatalysts with high activity and selective oxidation ability without side effects. Narrow band gap semiconductor photocatalyst such as In_2S_3, CdS and $AgInS_2$, which has higher negative conduction band (CB) position and lower valence band (VB) may be more appropriate for selective oxidation of alcohol to corresponding aldehyde. In recent years, narrow band gap semiconductor photocatalysts have been reported for the selective oxidation of alcohols [23,24]. At the same time, in order to increase the quantum efficiency, noble metal deposition, the addition of anion and transition metal ion, the composition of different semiconductors and surface photosensitization were widely used for the modification of the narrow-band photocatalysts [25–27]. It is known that In_2S_3 with band gap of 2.0–2.3 eV is a narrow band gap semiconductor, and the VB and CB are about 1.5 eV and $-0.5 \sim -1.0$ eV, respectively [28]. According to the reported result, it is concluded that In_2S_3 may be a suitable photocatalyst for the selective oxidation of alcohols [29]. However, to the best of our knowledge, there is no report on the selective oxidation of aromatic alcohols to corresponding aromatic aldehydes under visible light irradiation.

In the paper, In_2S_3 microsphere with a band gap of 1.96 eV was prepared using $InCl_3{\cdot}4H_2O$ and CH_3CSNH_2 as precursors. The structure and optical properties of In_2S_3 photocatalyst were investigated in detail. In_2S_3 microsphere shows an excellent photocatalytic performance in the conversion of aromatic alcohols to corresponding aromatic aldehydes. $\cdot O_2^-$ and $\cdot OH$ are the important oxidizing agents in the photocatalytic process. The possible mechanism for the conversion of aromatic alcohols to corresponding aromatic aldehydes was proposed.

2. Experimental

2.1. Materials

Indium chloride tetrahydrate ($InCl_3{\cdot}4H_2O$), thiacetamide (CH_3CSNH_2), hydrochloric acid (HCl) and other chemicals used in the experiments are of analytical reagent grade and were supplied by Shanghai Chemical Reagent Co. Ltd. of China without further purification. Distilled water was used in the experiments.

2.2. Preparation

In_2S_3 microspheres were prepared according to the following procedure. 1.0 mmol $InCl_3{\cdot}4H_2O$ was first dissolved in deionized water in a Teflon liner with 100 ml capacity, the solution pH of indium chloride was regulated to about 1 by dropwising HCl to avoid indium chloride's hydrolysis. And then, 2.5 mmol CH_3CSNH_2 as the source of sulfur was added into the above solution, the pH was adjusted to 3 by adding deionized water under continuous magnetic stirring. The Teflon liner was transferred into a stainless steel autoclave and maintained 160 °C for 24 h. After cooling down to room temperature naturally, the jacinth products were collected and washed by deionized water and absolute ethyl alcohol 3 times, respectively. Finally, the obtained products were dried in air at 60 °C for 2 h [30].

2.3. Characterization

In order to determine the crystal phase composition and the crystallite size of the photocatalysts, X-ray diffraction (XRD) measurement was carried out at room temperature using a Bruker D8 advance X-ray powder diffractometer with Cu Kα radiation and a scanning speed of 3°/min. The accelerating voltage and emission current were 40 kV and 40 mA, respectively. The crystallite size was calculated by X-ray line broadening analysis using the Scherrer equation.

UV–vis diffuse reflectance spectroscopy (DRS) measurements were carried out using a Hitachi UV-365 spectrophotometer equipped with an integrating sphere attachment. The analysis range was from 200 to 800 nm, and $BaSO_4$ was used as a reflectance standard.

The microcrystalline structure and surface characteristics of the photocatalyst were also investigated by using (JEOL JSM-6610LV) scanning electron microscope (SEM).

Transmission electron microscopy (TEM) and high-resolution transmission electron microscopy (HR-TEM) images were performed with a JEOL-2010 transmission electron microscope, using an accelerating voltage of 200 kV.

N_2 adsorption–desorption isotherms and the Brunauer–Emmett–Teller (BET) surface areas were measured at 77.3 K using a Micromeritics ASAP 3020 system.

Photoluminescence emission spectra (PL) were recorded on a JASCO FP-6500 type fluorescence spectrophotometer over a wavelength range of 360–500 nm.

2.4. Photocatalytic activity test

The photocatalytic selective oxidation of aromatic alcohols to corresponding aromatic aldehydes was performed as follows. A mixture of alcohol (0.5 mmol) and 80 mg of catalyst was dissolved in the inert solvent of 15 ml benzotrifluoride (BTF). Because of BTF's nonreactivity and high solubility for molecular oxygen, it was chosen as a solvent [8,15,21,31–33]. The prepared solution was loaded into a 100 ml of Teflon-lined stainless steel autoclave with a pressure gage which can be very convenient for monitoring

the pressure in the autoclave. The illumination window on the top of the reactor is made of high strength quartz glass. The reaction apparatus is shown in Fig. 1. Before the reaction, the autoclave was filled with molecular oxygen at a pressure of 0.1 MPa, and the suspension was magnetically stirred for 30 min to reach adsorption–desorption equilibrium. A 300 W Xenon lamp (PLS-SXE 300C, Beijing Perfect light) with a maximum emission at about 470 nm was used as a visible light source. The wavelength of the visible light was controlled through a 420 nm cutoff filter ($\lambda > 420$ nm, Instrument Company of Nantong, China). The reaction temperature was controlled at about 70 °C. After the reaction, the mixture was centrifuged at 4000 rmp for 30 min to remove the catalyst particles. The obtained solution was analyzed by a Gas Chromatograph (FuLi-9790) equipped with a SE-30 capillary column (30 m, 0.53 mm, Lanzhou Atech Technologies Co. Ltd.).

Conversion of alcohol, yield of aldehyde, and selectivity for aldehyde were defined as the follows:

$$\text{Conversion } (\%) = [(C_0 - C_{\text{alcohol}})/C_0] \times 100 \quad (1)$$

$$\text{Yield } (\%) = C_{\text{aldehyde}}/C_0 \times 100 \quad (2)$$

$$\text{Selectively } (\%) = [C_{\text{aldehyde}}/(C_0 - C_{\text{alcohol}})] \times 100 \quad (3)$$

where C_0 is the initial concentration of alcohol, and C_{alcohol} and C_{aldehyde} are the concentration of the substrate alcohol and the corresponding aldehyde, respectively, at a certain time after the photocatalytic reaction.

3. Results and discussion

3.1. Characterization of In_2S_3 photocatalyst

3.1.1. XRD analysis

The XRD patterns of fresh In_2S_3 and used In_2S_3 microspheres of 5 times are displayed in Fig. 2. It can be seen that the XRD pattern of the used In_2S_3 is similar to that of the fresh In_2S_3, and they show good crystal structure because both of them are in good agreement with the standard XRD pattern of In_2S_3 (JCPDS No. 65-0459). The diffraction peaks at 2θ values of 14.2°, 23.4°, 27.5°, 28.8°, 33.3°, 36.4°, 41.2°, 43.7°, 47.8°, 50.0°, 53.7°, 56.1°, 56.7°, 59.5°, 65.0°, 66.7°, 70.0°, 76.6° correspond to the (111), (220), (311), (222), (400), (331),(422),(511), (440), (531),(620),(533), (622), (444), (642), (731), (800), (751) crystal faces of In_2S_3, respectively. According to Scherrer formula, the average crystallite sizes of the fresh and used In_2S_3 are 20.6 nm and 20.2 nm calculated from the (440) peak of the XRD pattern.

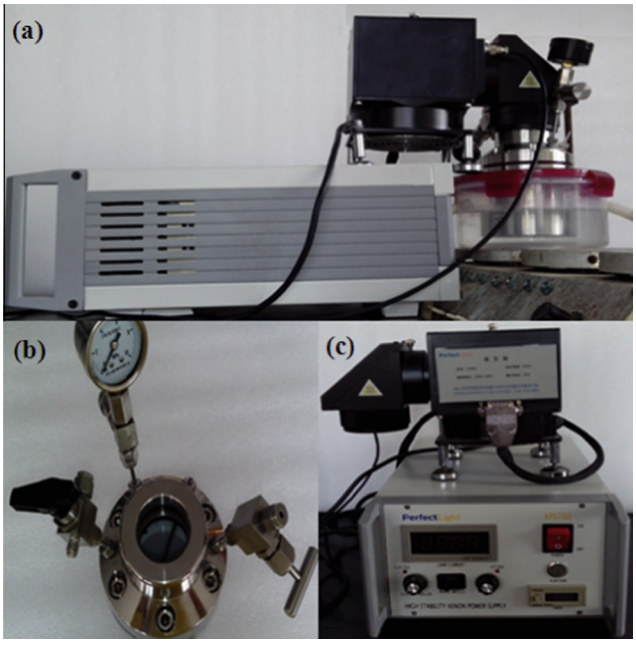

Fig. 1. The apparatus of photocatalytic reaction; (a) apparatus; (b) reactor and (c) light source.

3.1.2. UV–vis analysis

UV–vis diffuse reflectance spectra are always used to reveal the optical property of the as-prepared samples. Fig. 3 shows the UV–vis diffuse reflectance spectra of In_2S_3 sample. It is clear that the sample exhibits strong absorption in the visible region from 400 to 630 nm. The result is in accordance with the previous reports [30,34,35]. For an indirect-gap semiconductor, it is well known that the equation between the absorption coefficient and band gap energy can be described as follows: $(F(R)E)^2 = A(E-E_g)$ [30], where $F(R)$, E, A, E_g are diffuse reflection absorption coefficient, photon energy, proportionality constant, and optical band gap energy, respectively. From the equation, $(F(R)E)^2$ has a linear relation with E. We can get the band gap $E_g = 1.96$ eV of as-prepared In_2S_3 by extrapolating the linear relation to $(F(R)E)^2 = 0$. Therefore, In_2S_3 can absorb large amounts of visible light, and it may be a suitable visible-irradiation photocatalyst. The band positions of In_2S_3 can be calculated by the following empirical formulas [36]:

$$E_{VB} = X + 0.5E_g - E^e \quad (4)$$

$$E_{CB} = E_{VB} - E_g \quad (5)$$

where E_{VB} is the valence band potential; E_{CB} is the conduction band potential; X is the absolute electronegativity of the semiconductor; E^e is the energy of free electrons on the hydrogen scale ($E^e = 4.5$ eV). From the calculation, it is known that the absolute electronegativity of In_2S_3 is about 4.7 eV, so the E_{CB} and E_{VB} of In_2S_3 are −0.78 eV and 1.18 eV, respectively.

3.1.3. SEM, TEM, HRTEM and EDS analyses

The morphology and microstructure of the prepared In_2S_3 sample were characterized by SEM. The image is shown in Fig. 4(a). It is clear that the appearance of the sample displays a ball-like aggregate structure of varying sizes with diameter around 1–3 μm. The aggregates consist of many small crystal particles. The TEM and HRTEM analysis has been performed to study the morphologies of In_2S_3 sample. Fig. 4(b) shows TEM image of the sample. It can be seen that the sample shows a loose nanosheets structure. The triangular and polygonal boundaries of nanosheets interpenetrate each other to display their very small thickness. A HRTEM image shown in Fig. 4(c) reveals In_2S_3 sample's growth direction. The crystal lattice diameter of 0.622 nm, 0.311 nm, 0.267 nm corresponds to the (111), (222) and (400) crystallographic planes of In_2S_3 microsphere, respectively, which further confirmed the high crystallinity of the sample. The chemical composition of the sample can be tested by using energy-dispersive spectroscopy (EDS). A representative EDS spectrum displayed in Fig. 4(d) reveals that the In/S atomic percentage ratio equals to the mean value of 2:3, which is close to the stoichiometry of In_2S_3 sample.

3.1.4. N_2 adsorption–desorption analysis

The nitrogen adsorption–desorption isotherms of In_2S_3 microsphere are shown in Fig. 5. It is clear that the sample exhibits type IV isotherms with a typical H3 hysteresis loop characteristic of mesoporous solids according to the IUPAC classification [37]. Type IV isotherm is a special type of isotherm which reflects the results

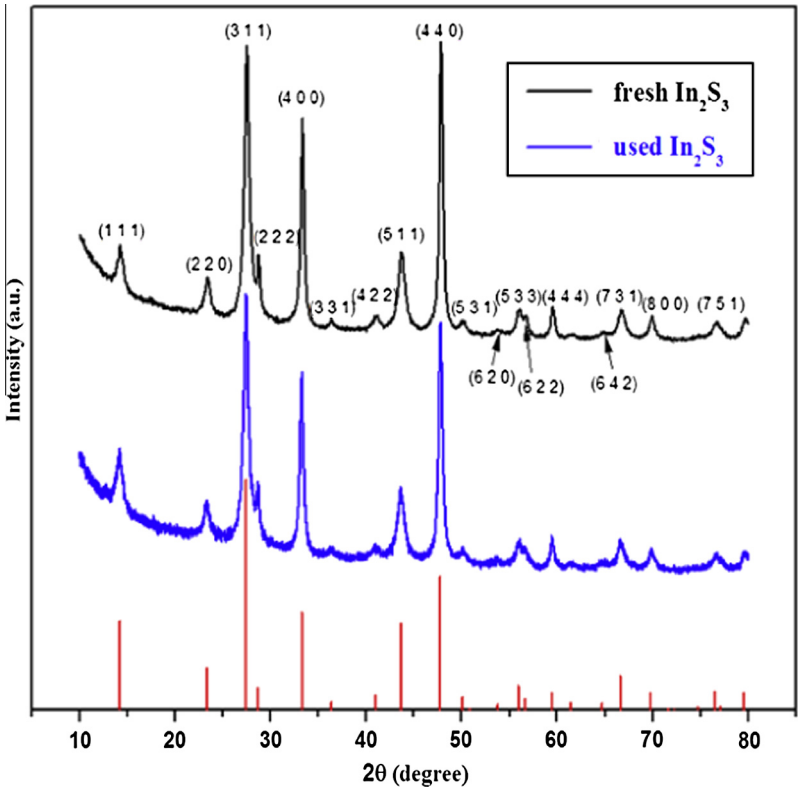

Fig. 2. XRD patterns of the fresh and used In_2S_3 and standard XRD pattern of In_2S_3 (JCPDS No. 65-0459).

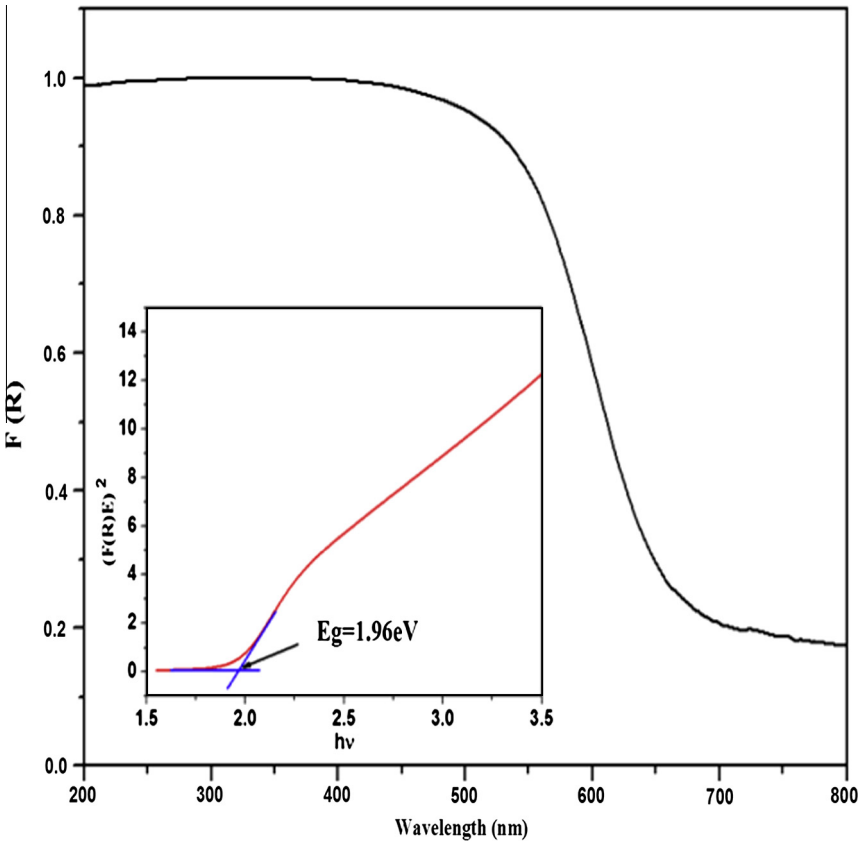

Fig. 3. UV–vis diffuse reflectance spectra of In_2S_3 photocatalyst.

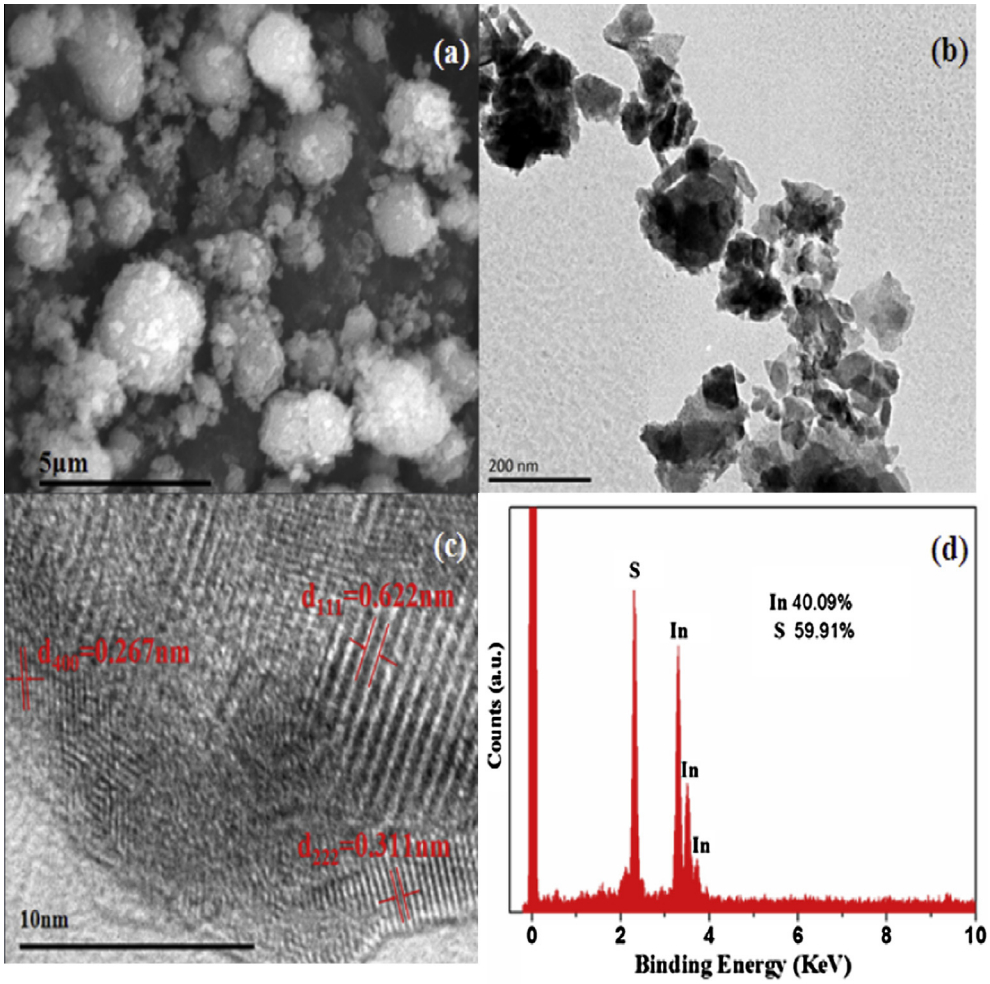

Fig. 4. SEM (a), TEM (b), HRTEM (c), EDS (d) of In_2S_3 photocatalyst.

of harmonic type multilayer adsorption evenly on the surface of solid. The type H3 hysteresis loop is observed with aggregates of plate-like particles giving rise to slit-shaped pores.

The corresponding pore size distribution of In_2S_3 microsphere is shown in the inset of Fig. 5. The pore width of In_2S_3 sample is about 3.7 nm obtained from the desorption branch of the isotherm. The BET surface area of In_2S_3 sample is measured to be ca.47.4 m^2/g.

3.2. Evaluation of photocatalytic activity

Fig. 6 shows the photocatalytic performance of selective oxidation of a range of alcohols to corresponding aldehydes under visible light irradiation. It is clear that the conversion of the alcohols increases constantly with the increase of the reaction time. Similarly, the yield of the corresponding aldehydes also rises with the extension of irradiation time. For example, for the selective oxidation of benzyl alcohol, when the illumination time is 1, 2 and 4 h, the conversion is 8.4%, 17.4% and 41.5%, and the yield is 8.4%, 17.4% and 41.4%, respectively. So the selectivity is about 100%. From Fig. 6, it also can be seen that the selectivity of the reactions for the alcohols is very high except cinnamyl alcohol. It has been reported that the selectivity is related to the electronegativity of functional group [33,38]. In general, the stronger the electronegativity, the easier the oxidation. It is known that the electronic effect of the functional group is as follows: $-OCH_3$ > –H > –Cl > –F > $-NO_2$, so the selectivity of the reaction should be as follows: benzyl alcohol = p-methoxybenzyl alcohol > p-chlorobenzyl alcohol > p-fluorobenzyl alcohol > p-nitrobenzyl alcohol. In the study, the results prove the above analysis. However, for allylic alcohol, such as cinnamyl alcohol (Fig. 6f), the selectivity is relatively low. This may result from π–π conjugated effect, which is caused by the formation of benzene ring and C=C double bond, and then the π–π conjugated effect influences the oxidation process of cinnamyl alcohol.

In order to investigate the solvent on the effect of selective oxidation of alcohols to corresponding aldehydes, the solvents such as benzotrifluoride, toluene, aceonitrile and water were selected. The result is shown in Fig. 7. It is clearly seen that the conversion of benzyl alcohol to benzaldehyde in BTF solvent is higher than that in nonfluorinated solvents such as toluene, aceonitrile and water. When illuminated for 4 h, the selectivity is 99.8% in the BTF solution, 66.2% in the toluene, 8.1% in the aceonitrile, and 1.1% in the water solution. It is clear that the selectivity of benzaldehyde decreases with the rise of solvent's polarity (water > aceonitrile > toluene) because of the solubleness of O–O bands in the polar solution [33,38], and this phenomenon can be attributed to benzotrifluoride which can dissolve more oxygen [8,31].

From Fig. 7, it also can be seen that when water was selected as a solvent, the selectivity and yield are the lowest while the conversion is the highest among the four solvents. It is clear that many intermediate products will be produced in the reaction process. The kinds and quantity of the intermediate products are being investigated in our laboratory.

In addition, some blank tests were conducted in order to detect whether benzaldehyde is produced when one or two experimental

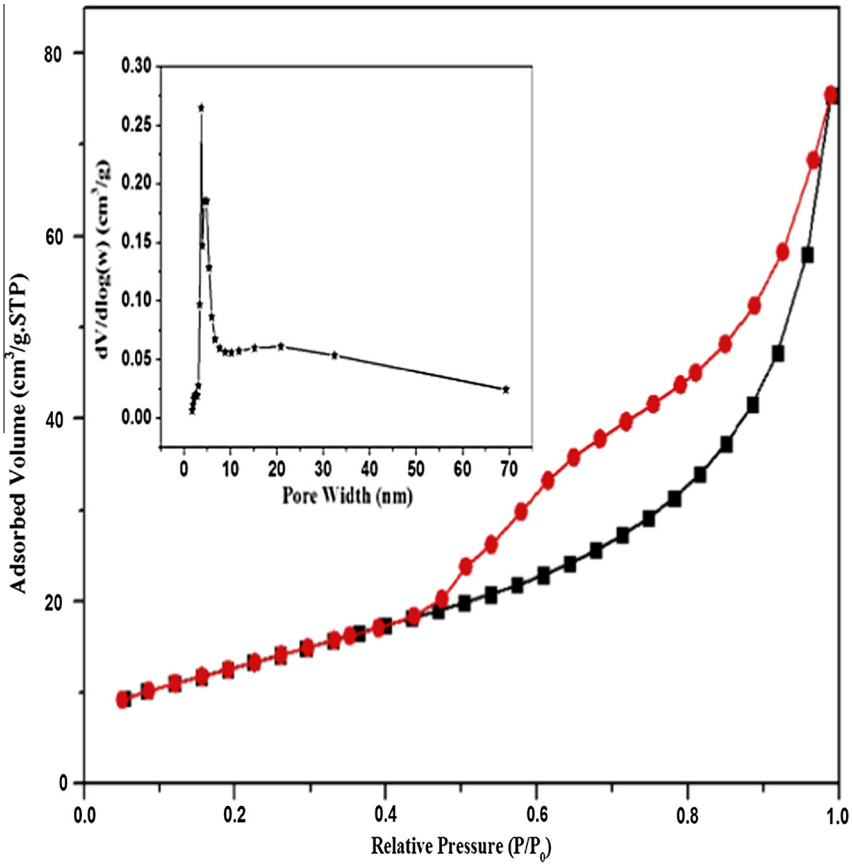

Fig. 5. N_2 adsorption–desorption isotherm and the pore size distribution curves (inset) of In_2S_3 microsphere.

conditions have changed. The result shows that no conversion of benzyl alcohol is detected in the blank experiments performed in the absence of catalyst and/or visible light, which ensures that the reaction is a photocatalytic process. Furthermore, the trace conversion of benzyl alcohol is demonstrated in the controlled experiment carried out in the presence of nitrogen, revealing that oxygen is indispensable as primary oxidant during the photocatalytic process under such ambient conditions. In other words, the oxidation reaction of alcohols to corresponding aldehydes proceeds successfully owing to the participation of catalyst, oxygen, and the visible light irradiation. It is proved that this is a process of photocatalytic oxidation with oxygen existence.

The cyclic experiments were carried out under the same conditions using In_2S_3 microsphere as a photocatalyst in order to determine the stability of the photocatalyst. The results are shown in Fig. 8. It is clear that in the 5-cycle experiments, the conversion of the benzyl alcohol and yield of benzaldehyde do not change obviously. And the stability of In_2S_3 microsphere also can be found from the XRD pattern. It is clear that XRD patterns of the fresh and used In_2S_3 samples for 5 times do not have any change (See Fig. 2). Therefore, it can be concluded that the In_2S_3 photocatalyst has good stability in the experimental conditions. It is proposed that good stability of In_2S_3 photocatalyst may be attributed to the reaction system composed of organic solvents, which reduces the photocorrosion to the In_2S_3 photocatalyst.

3.3. Possible photocatalytic mechanism

3.3.1. Role of the reactive species

It is well known that the $\cdot O_2^-$, h^+ and ·OH are the primary reactive species for the photocatalytic oxidation. The scavenger study was carried out in order to discriminate the roles of the reactive species from each other. The function of these reactive species in the photocatalytic process based on the change of the catalytic activity can be realized by adding different scavengers respectively to eliminate the corresponding reactive species. In this experiment, p-benzoquinone (BQ) was introduced as the quencher of $\cdot O_2^-$, isopropyl alcohol (IPA) was adopted to quench ·OH, and oxalic acid (OA) was added to the reaction system as an h^+ quencher [39,40].

The result is shown in Fig. 9. It is clear that when the BQ and IPA were added into the reaction system, the yield of benzaldehyde is decreased obviously. Adding BQ, the yield decreases from 41.4% to 18.8%, and adding IPA, the yield decreases from 41.4% to 33.6%. However, the yield of benzaldehyde was not obviously changed when OA was added to the reaction system. Furthermore, using triethanolamine and methanol as the h^+ quencher, the result was the same as that of adding OA. Based on the results, it could be concluded that the $\cdot O_2^-$ and ·OH, rather than the h^+, are the major reactive species in the photocatalytic reaction system.

In order to determine the presence of the $\cdot O_2^-$ and ·OH in the reaction system, the following experiments were carried out. The photoluminescence (PL) technique with terephthalic acid (TA) as the indicator was used to confirm whether there is the generation of hydroxyl radicals in the reaction system. TA can react with ·OH to produce 2-hydroxyterephthalic acid (HTA) which has high fluorescence during the photocatalytic process, and the PL peak intensity is in proportion to the amount of ·OH radicals formed in the water. The mechanism is shown in Scheme 1. Experimental procedures were reported in the early reports [41]. The result is shown in Fig. 10. It is clear that there is an obvious PL signal after 4 h of visible light irradiation. It proves that ·OH is produced in the photocatalytic oxidation process.

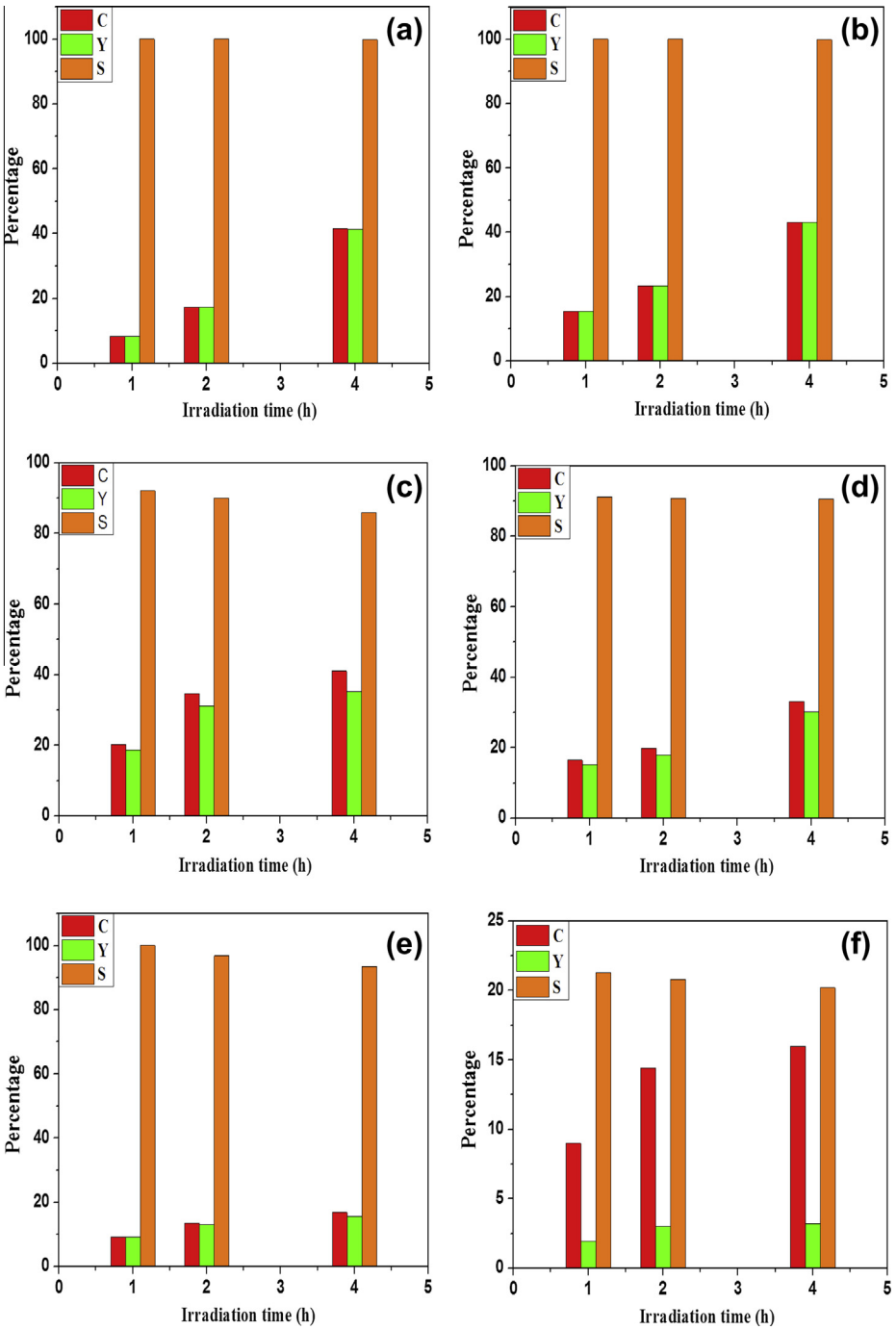

Fig. 6. Photocatalytic performance of selective oxidation of a range of alcohols to corresponding aldehydes using In_2S_3 photocatalyst under visible light irradiation (a) benzyl alcohol; (b) p-methoxybenzyl alcohol; (c) p-chlorobenzyl alcohol; (d) p-fluorobenzyl alcohol; (e) p-nitrobenzyl alcohol; (f) cinnamyl alcohol. In figures, C means conversion, Y means yield and S means selectively.

Nitroblue tetrazolium (NBT, 2.5×10^{-5} mol/L, exhibiting an absorption maximum at 259 nm) was used to check whether there is $\cdot O_2^-$ generated from In_2S_3 photocatalytic system[42,43]. Because NBT can react with $\cdot O_2^-$, the production of $\cdot O_2^-$ can be analyzed by UV–vis absorption spectra of nitroblue tetrazolium before and after reaction. From Fig. 11, it is clear that the absorbance decreases greatly from 1.448 down to 0.336, which demonstrates that the concentration of NBT in the reaction system was reduced greatly. Obviously, $\cdot O_2^-$ was produced in the photocatalytic oxidation process. So it is in agreement with the experimental result of the reactive species.

It is known that the photocatalytic oxidation and reduction abilities of semiconductors were determined by the potentials of valence and conduction bands. The forbidden band width of In_2S_3 is 1.96 eV, and the CB and VB potentials of In_2S_3 are −0.78 eV and 1.18 eV, respectively. The photoexcited electrons in the CB of In_2S_3 can reduce O_2 to give $\cdot O_2^-$ and $\cdot HO_2$, because the CB edge potential of In_2S_3 (−0.78 eV vs. NHE) is more negative than the standard redox potentials of $E^{\Theta}(O_2/\cdot O_2^-)$ (−0.33 eV vs. NHE) and $E^{\Theta}(O_2/\cdot HO_2)$ (−0.05 eV vs. NHE). And the photoexcited holes in the VB of In_2S_3 cannot oxidize OH^- to give $\cdot OH$ because the VB potential of In_2S_3 is more negative than the standard redox potential

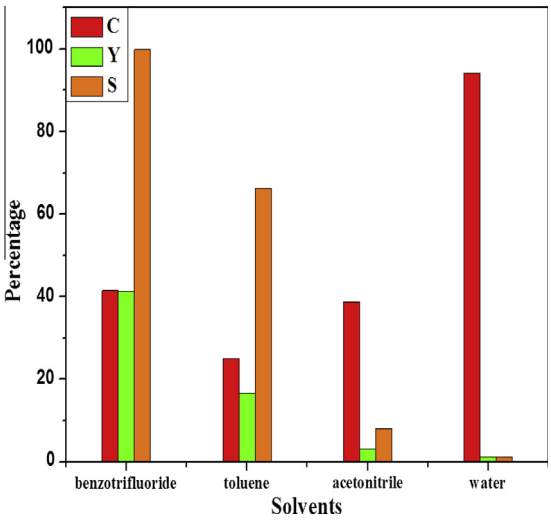

Fig. 7. Photocatalytic selective oxidation of benzyl alcohol to benzaldehyde using In_2S_3 under the visible light irradiation ($\lambda \geqslant 420$ nm) for 4 h in different solvents.

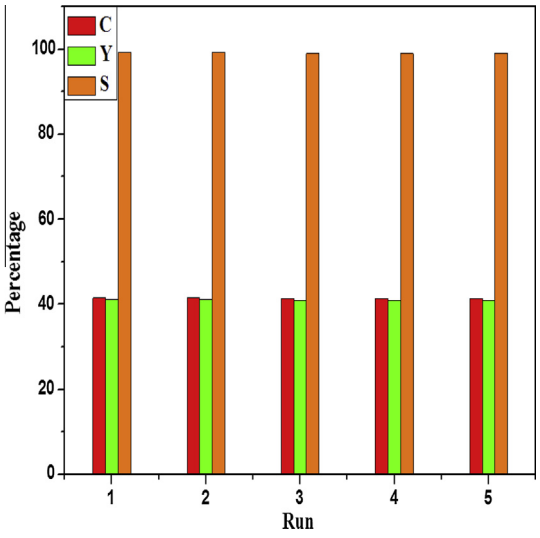

Fig. 8. Cyclic experiments of In_2S_3 microsphere photocatalyst.

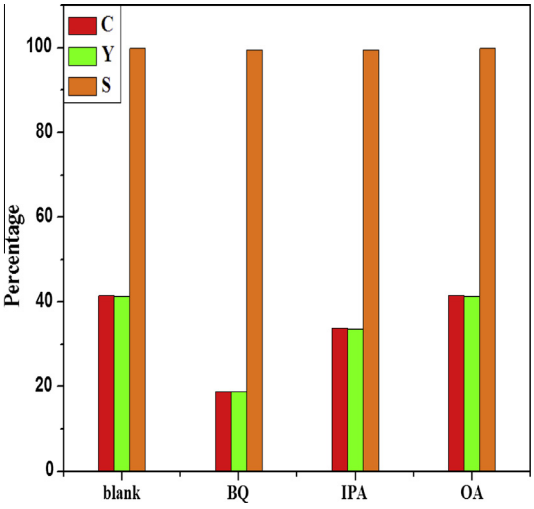

Fig. 9. Effects of a series of scavengers on the selective oxidation of benzyl alcohol (The dosage of scavengers = 0.1 mmol/L, illumination time t = 4 h).

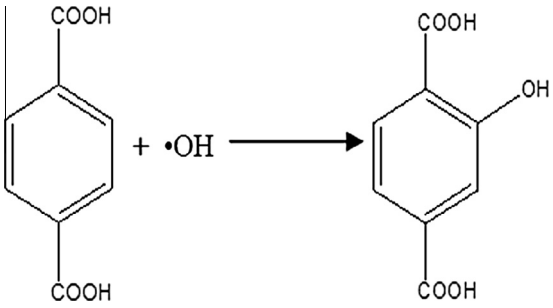

Scheme 1. Reaction between terephthalic acid (TA) and ·OH.

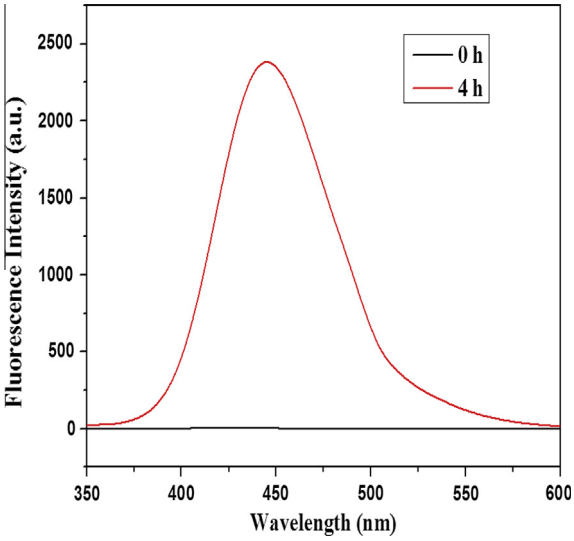

Fig. 10. Photoluminescence emission spectra of the In_2S_3 sample.

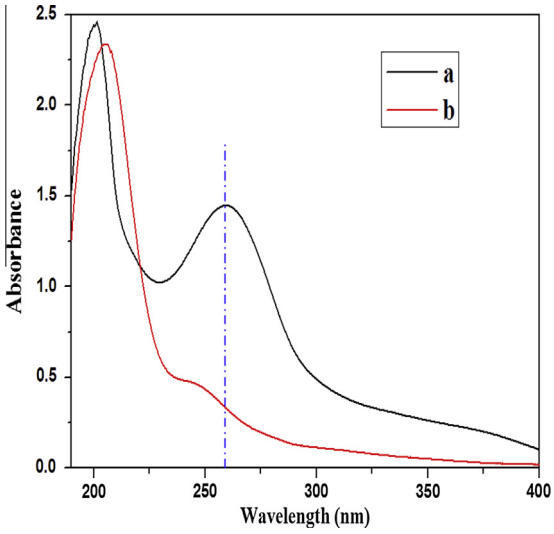

Fig. 11. The absorbance of nitroblue tetrazolium before visible light irradiation (a) and after visible light irradiation for 4 h (b).

of $OH^-/{\cdot}OH$ ($E^{\Theta}(OH^-/{\cdot}OH) = 2.4$ eV) [44]. However, the result of ·OH experiment shows that the ·OH can be produced in the reaction system of In_2S_3 photocatalyst. It is suggested that the ·OH may be produced from the $\cdot O_2^-$, which is another source of ·OH [44].

$$e^- + O_2 \rightarrow \cdot O_2^- \quad (6)$$

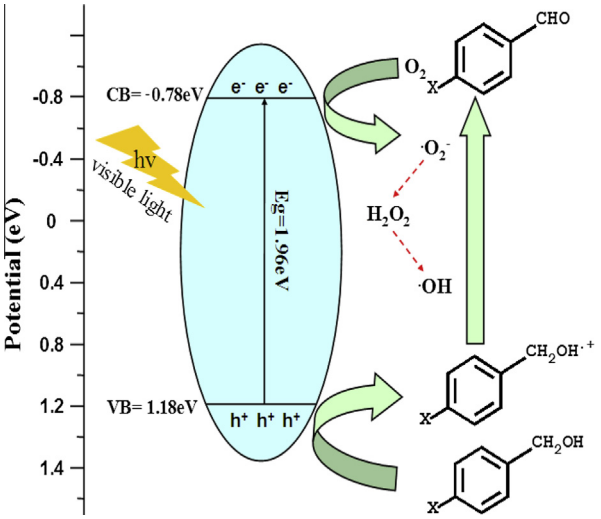

Fig. 12. Proposed mechanism of selective oxidation of aromatic alcohols to corresponding aromatic aldehydes using In_2S_3 under visible light irradiation.

$$\cdot O_2^- + e^- + 2H^+ \rightarrow H_2O_2 \quad (7)$$

$$\cdot O_2^- + H_2O_2 \rightarrow \cdot OH + OH^- + O_2 \quad (8)$$

$$H_2O_2 \rightarrow 2\cdot OH \quad (9)$$

3.3.2. Reaction mechanisms

On the basis of the above results and analysis, a possible pathway of selective oxidation of aromatic alcohols to corresponding aromatic aldehydes using In_2S_3 catalysts under visible light can be proposed. Firstly, In_2S_3 catalysts are excited under visible light and produce plenty of holes and electrons. The aromatic alcohol in the solution interacts with holes to form the corresponding radical cation. The electrons on the conduction band can be captured by electrophilic O_2, generating $\cdot O_2^-$. And then $\cdot O_2^-$ oxidizes radical cation to produce aromatic aldehydes. At this time, aromatic alcohols release H^+ in the oxidization process, then 2 mol H^+ will react with 1 mol $\cdot O_2^-$ and 1 mol electrons to produce 1 mol H_2O_2 which decompose 2 mol ·OH. Lastly, $\cdot O_2^-$ and ·OH can oxidize radical cation to corresponding aromatic aldehydes simultaneously. This reaction process can be displayed in Fig. 12.

4. Conclusions

In summary, In_2S_3 microsphere photocatalyst with E_{CB} of −0.78 eV and E_{VB} of 1.18 eV was prepared by hydrothermal method. The photocatalyst presents fine conversion and selectivity for selective oxidation of aromatic alcohols to corresponding aromatic aldehydes under the visible light irradiation, and it has a good stability. The conversion of benzyl alcohol reaches to 41.5%, and the yield of benzaldehyde is 41.4% after being illuminated for 4 h. When the catalyst, oxygen and the visible light irradiation are present, the selective oxidation of aromatic alcohols is able to proceed. $\cdot O_2^-$ and ·OH are the important oxidizing agents in the reaction system. The selectivity of the reaction is as follows: benzyl alcohol = p-methoxybenzyl alcohol > p-chlorobenzyl alcohol > p-fluorobenzyl alcohol > p-nitrobenzyl alcohol.

Acknowledgement

This study was supported by the Natural Science Foundation of China (NSFC, grant Nos. 51172086, 21103060 and 51272081).

References

[1] G. Palmisano, S. Yurdakal, V. Augugliaro, V. Loddo, L. Palmisano, Photocatalytic selective oxidation of 4-methoxybenzyl alcohol to aldehyde in aqueous suspension of home-prepared titanium dioxide catalyst, Pure Appl. Chem. 349 (2007) 964–970.
[2] F.Z. Su, S.C. Mathew, G. Lipner, X.Z. Fu, M. Antonietti, S. Blechert, X.C. Wang, Mpg-C_3N_4-catalyzed selective oxidation of alcohols using O_2 and visible light, J. Am. Chem. Soc. 132 (2010) 16299–16301.
[3] S. Yurdakal, G. Palmisano, V. Loddo, V. Augugliaro, L. Palmisano, Nanostructured rutile TiO_2 for selective photocatalytic oxidation of aromatic alcohols to aldehydes in water, J. Am. Chem. Soc. 130 (2008) 1568–1569.
[4] U.R. Pillai, E. Sahle-Demessie, Oxidation of alcohols over Fe^{3+}/montmorillonite-K10 using hydrogen peroxide, Appl. Catal. A: Gen. 245 (2003) 103–109.
[5] W.P. Griffith, J.M. Jolliffe, Ruthenium and Osmium carboxylato oxo complexes as organic oxidants, Stud. Surf. Sci. Catal. 66 (1991) 395–400.
[6] W.Z. Chen, F.N. Rein, R.C. Rocha, Homogeneous photocatalytic oxidation of alcohols by a chromophore-catalyst dyad of ruthenium complexes, Angew. Chem. Int. Ed. 48 (2009) 9672–9675.
[7] S. Higashimoto, N. Kitao, N. Yoshida, T. Sakura, M. Azuma, H. Ohue, Y. Sakata, Selective photocatalytic oxidation of benzyl alcohol and its derivatives into corresponding aldehydes by molecular oxygen on titanium dioxide under visible light irradiation, J. Catal. 266 (2009) 279–285.
[8] M. Zhang, C.C. Chen, W.H. Ma, J.C. Zhao, Visible-light-induced aerobic oxidation of alcohols in a coupled photocatalytic system of dye-sensitized TiO_2 and TEMPO, Angew. Chem. Int. Ed. 47 (2008) 9730–9733.
[9] X.Y. Zhang, H.P. Li, X.L. Cui, Y.H. Lin, Graphene/TiO_2 nanocomposites: synthesis, characterization and application in hydrogen evolution from water photocatalytic splitting, J. Mater. Chem. 20 (2010) 2801–2806.
[10] Z.Y. Liu, X.T. Zhang, S. Nishimoto, T. Murakami, A. Fujishima, Efficient photocatalytic degradation of gaseous acetaldehyde by highly ordered TiO_2 nanotube arrays, Environ. Sci. Technol. 42 (2008) 8547–8551.
[11] W. Choi, A. Termin, M.R. Hoffmann, The role of metal ion dopants in quantum-sized TiO_2: Correlation between photoreactivity and charge carrier recombination dynamics, J. Phys. Chem. 98 (1994) 13669–13679.
[12] K. Naoi, Y. Ohko, T. Tatsuma, TiO_2 films loaded with silver nanoparticles: control of multicolor photochromic behavior, J. Am. Chem. Soc. 126 (2004) 3664–3668.
[13] A. Zaban, O.I. Mićić, B.A. Gregg, A.J. Nozik, Photosensitization of nanoporous TiO_2 electrodes with InP quantum dots, Langmuir 14 (1998) 3153–3156.
[14] J.K. Zhou, L. Lv, J.Q. Yu, H.L. Li, P.Z. Guo, H. Sun, X.S. Zhao, Synthesis of self-organized polycrystalline F-doped TiO_2 hollow microspheres and their photocatalytic activity under visible light, J. Phys. Chem. C 112 (2008) 5316–5321.
[15] Y.H. Zhang, Z.R. Tang, X.Z. Fu, Y.J. Xu, Engineering the unique 2D mat of graphene to achieve graphene–TiO_2 nanocomposite for photocatalytic selective transformation: what advantage does graphene have over its forebear carbon nanotube?, ACS Nano 5 (2011) 7426–7435
[16] N. Zhang, S.Q. Liu, X.Z. Fu, Y.J. Xu, Synthesis of M@TiO_2 (M = Au, Pd, Pt) core–shell nanocomposites with tunable photoreactivity, J. Phys. Chem. C 115 (2011) 9136–9145.
[17] C.J. Li, G.R. Xu, B.H. Zhang, J.R. Gong, High selectivity in visible-light-driven partial photocatalytic oxidation of benzyl alcohol into benzaldehyde over single-crystalline rutile TiO_2 nanorods, Appl. Catal. B: Environ. 115–116 (2012) 201–208.
[18] X.G. Wang, H. Kawanami, S.E. Dapurkar, N.S. Venkataramanan, M. Chatterjee, T. Yokoyama, Y. Ikushima, Selective oxidation of alcohols to aldehydes and ketones over TiO_2-supported gold nanoparticles in supercritical carbon dioxide with molecular oxygen, Appl. Catal. A: Gen. 349 (2008) 86–90.
[19] J. Zhang, Y. Nosaka, Quantitative detection of OH radicals for investigating the reaction mechanism of various visible-light TiO_2 photocatalysts in aqueous suspension, J. Phys. Chem. C 117 (2013) 1383–1391.
[20] N. Zhang, S.Q. Liu, X.Z. Fu, Y.J. Xu, A simple strategy for fabrication of "Plum-Pudding" type Pd@CeO_2 semiconductor nanocomposite as a visible-light-driven photocatalyst for selective oxidation, J. Phys. Chem. C 115 (2011) 22901–22909.
[21] N. Zhang, X.Z. Fu, Y.J. Xu, A facile and green approach to synthesize Pt@CeO_2 nanocomposite with tunable core–shell and yolk–shell structure and its application as a visible light photocatalyst, J. Mater. Chem. 21 (2011) 8152.
[22] A. Tanaka, K. Hashimoto, H. Kominami, Preparation of Au/CeO_2 exhibiting strong surface plasmon resonance effective for selective or chemoselective oxidation of alcohols to aldehydes or ketones in aqueous suspensions under irradiation by green light, J. Am. Chem. Soc. 134 (2012). 14526–1453.
[23] S. Farhadi, M. Zaidi, Polyoxometalate–zirconia (POM/ZrO2) nanocomposite prepared by sol-gel process: a green and recyclable photocatalyst for efficient and selective aerobic oxidation of alcohols into aldehydes and ketones, Appl. Catal. A: Gen. 354 (2009) 119–126.
[24] Z.X. Chen, J.J. Xu, Z.Y. Ren, Y.H. He, G.C. Xiao, High efficient photocatalytic selective oxidation of benzyl alcohol to benzaldehyde by solvothermal-synthesized $ZnIn_2S_4$ microspheres under visible light irradiation, J. Solid State Chem. 205 (2013) 134–141.
[25] M.R. Bayati, A.Z. Moshfegh, F. Golestani-Fard, Synthesis of narrow band gap $(V_2O_5)_x$-$(TiO_2)_{1-x}$ nano-structured layers via micro arc oxidation, Appl. Surf. Sci. 256 (2010) 2903–2909.

[26] L. Chen, S.F. Yin, R. Huang, Y. Zhou, S.L. Luo, C.-T. Au, Facile synthesis of BiOCl nano-flowers of narrow band gap and their visible-light-induced photocatalytic property, Chem. Commun. 23 (2012) 54–57.
[27] Y.L. Min, K. Zhang, Y.C. Chen, Y.G. Zhang, Synthesis of novel visible light responding vanadate/TiO_2 heterostructure photocatalysts for application of organic pollutants, Chem. Eng. J. 175 (2011) 76–83.
[28] X.Q. An, J.C. Yu, F. Wang, C.H. Li, Y.C. Li, One-pot synthesis of In_2S_3 nanosheets/graphene composites with enhanced visible-light photocatalytic activity, Appl. Catal. B: Environ. 129 (2013) 80–88.
[29] X.Y. Xiao, J. Jiang, L.Z. Zhang, Selective oxidation of benzyl alcohol into benzaldehyde over semiconductors under visible light: The case of $Bi_{12}O_{17}Cl_2$ nanobelts, Appl. Catal. B: Environ. 142–143 (2013) 487–493.
[30] Y.H. He, D.Z. Li, G.C. Xiao, W. Chen, Y.B. Chen, M. Sun, H.J. Huang, X.Z. Fu, A new application of nanocrystal In_2S_3 in efficient degradation of organic pollutants under visible light irradiation, J. Phys. Chem. C 113 (2009) 5254–5262.
[31] M. Zhang, Q. Wang, C.C. Chen, L. Zang, W.H. Ma, J.C. Zhao, Oxygen atom transfer in the photocatalytic oxidation of alcohols by TiO_2: oxygen isotope studies, Angew. Chem. Int. Ed. 48 (2009) 6081–6084.
[32] N. Zhang, S.Q. Liu, X.Z. Fu, Y.J. Xu, Fabrication of coenocytic Pd@CdS nanocomposite as a visible light photocatalyst for selective transformation under mild conditions, J. Mater. Chem. 22 (2012) 5042.
[33] N. Zhang, Y.H. Zhang, X.Y. Pan, X.Z. Fu, S.Q. Liu, Y.J. Xu, Assembly of CdS nanoparticles on the two-dimensional graphene scaffold as visible-light-driven photocatalyst for selective organic transformation under ambient conditions, J. Phys. Chem. C 115 (2011) 23501–23511.
[34] X.L. Fu, X.X. Wang, Z.X. Chen, Z.Z. Zhang, Z.H. Li, D.Y.C. Leung, L. Wu, X.Z. Fu, Photocatalytic performance of tetragonal and cubic β-In_2S_3 for the water splitting under visible light irradiation, Appl. Catal. B: Environ. 95 (2010) 393–399.
[35] S. Rengaraj, S. Venkataraj, C.-W. Tai, Y. Kim, E. Repo, M. Sillanpää, Self-assembled mesoporous hierarchical-like In_2S_3 hollow microspheres composed of nanofibers and nanosheets and their photocatalytic activity, Langmuir 27 (2011) 5534–5541.
[36] Z.W. Mei, S.X. Ouyang, D.M. Tang, T. Kako, D. Golbergc, J.H. Ye, An ion-exchange route for the synthesis of hierarchical $In_2S_3/ZnIn_2S_4$ bulk composite and its photocatalytic activity under visible-light irradiation, Dalton Trans. 42 (2013) 2687–2690.
[37] K.S.W. Sing, D.H. Everett, R.A.W. Haul, L. Moscou, R.A. Pierotti, J. Rouquérol, T. Siemieniewska, Reporting physisorption data for gas/sold systems with special reference to the determination of surface area and porosity, Pure Appl. Chem. 57 (1985) 603–619.
[38] T. Punniyamurthy, S. Velusamy, J. Iqbal, Recent advances in transition metal catalyzed oxidation of organic substrates with molecular oxygen, Chem. Rev. 105 (2005) 2329–2363.
[39] S. Chen, Y. Hu, S. Meng, X. Fu, Study on the separation mechanisms of photogenerated electrons and holes for composite photocatalysts g-C_3N_4-WO_3, Appl. Catal. B: Environ. 150–151 (2014) 564–573.
[40] W.J. Wang, L.Z. Zhang, T.C. An, G.Y. Li, H.Y. Yip, P.K. Wong, Comparative study of visible-light-driven photocatalytic mechanisms of dye decolorization and bacterial disinfection by B–Ni-codoped TiO_2 microspheres: the role of different reactive species, Appl. Catal. B: Environ. 108–109 (2011) 108–116.
[41] X.L. Fu, Y.F. Hu, Y.G. Yang, W. Liu, S.F. Chen, Ball milled h-BN: an efficient holes transfer promoter to enhance the photocatalytic performance of TiO_2, J. Hazard. Mater. 244–245 (2013) 102–110.
[42] L.Q. Ye, J.Y. Liu, Z. Jiang, T.Y. Peng, L. Zan, Facets coupling of BiOBr-g-C_3N_4 composite photocatalyst for enhanced visible-light-driven photocatalytic activity, Appl. Catal. B: Environ. 142–143 (2013) 1–7.
[43] L.Q. Ye, J.N. Chen, L.H. Tian, J.Y. Liu, T.Y. Peng, K.J. Deng, L. Zan, BiOI thin film via chemical vapor transport: Photocatalytic activity, durability, selectivity and mechanism, Appl. Catal. B: Environ. 130–131 (2013) 1–7.
[44] W.J. Li, D.Z. Li, Y.M. Lin, P.X. Wang, W. Chen, X.Z. Fu, Y. Shao, Evidence for the active species involved in the photodegradation process of methyl orange on TiO_2, J. Phys. Chem. C 116 (2012) 3552–3560.